Fluorescence Stopped-Flow Kinetics of the Cleavage of Synthetic Oligodeoxynucleotides by the *Eco*RI Restriction Endonuclease†

Jürgen Alves,* Claus Urbanke, Anja Fliess, Günter Maass, and Alfred Pingoud
Zentrum Biochemie, Medizinische Hochschule Hannover, Konstanty-Gutschow-Strasse 8, D-3000 Hannover 61, West Germany
Received January 13, 1989; Revised Manuscript Received June 6, 1989

ABSTRACT: We have investigated in fluorescence stopped-flow and temperature-jump experiments the *Eco*RI-catalyzed cleavage of synthetic palindromic tridecadeoxynucleotides which contain the *Eco*RI site but differ in the flanking sequences. The overall reaction can be resolved in several reactions which were analyzed by a nonlinear least-squares fitting procedure on the experimental data. The result of this analysis is a minimal scheme that describes the overall reaction in terms of the rate constants of the individual reactions. According to this scheme *Eco*RI and the tridecadeoxynucleotide substrates associate in the presence of Mg^{2+} in a nearly diffusion-controlled process. This is followed by a reaction which is or includes the cleavage of the first phosphodiester bond. There is no indication for a time-resolved conformational transition prior to catalysis. After cleavage of the first strand, dissociation of the nicked double strand can occur, which then rearranges to the original palindromic double-stranded substrate and is bound again by the enzyme. Alternatively, the nicked double strand can be cleaved in the second strand. This reaction is followed by product release from the enzyme. The magnitude of the individual rate constants depends on the substrate used; the differences explain the preference of *Eco*RI for substrates that contain AT as compared to GC base pairs next to the recognition site.

*Eco*RI is a class II restriction endonuclease which recognizes the sequence

```
-G↓AATTC-
-CTTAA↑G-
```

and in the presence of Mg^{2+} ions cleaves the DNA at the indicated positions [Hedgepeth et al., 1972; for review, cf. Modrich and Roberts (1982)]. It binds to DNA nonspecifically (Goppelt et al., 1980; Woodhead & Malcolm, 1980; Langowski et al., 1980; Terry et al., 1983) and makes use of linear diffusion to find its target site (Jack et al., 1982; Ehbrecht et al., 1985; Terry et al., 1985). The specific interaction at the recognition site leads to a distortion of the regular B-DNA conformation within this site (Frederick et al., 1984; Kim et al., 1984), thereby increasing the width of the major groove, in which most of the recognition elements are located (Lu et al., 1981; Fliess et al., 1986; Brennan et al., 1986; McClarin et al., 1986; Seela & Kehne, 1987; McLaughlin et al., 1987). The rate of phosphodiester bond cleavage is influenced by the sequence flanking the recognition site (Thomas & Davis, 1975; Goldstein et al., 1975; Forsblom et al., 1976; Rubin & Modrich, 1978; Halford et al., 1980; Berkner & Folk, 1983; Alves et al., 1984). It is the rate-determining step under conditions where the enzyme is not trapped in nonspecific binding (Langowski et al., 1981). Furthermore, under certain reaction conditions a nicked intermediate can accumulate before double-strand cleavage is complete (Modrich & Zabel, 1976; Ruben et al., 1977; Rubin & Modrich, 1978; Halford et al., 1979).

So far the individual reaction steps characterizing the binding, recognition, and cleavage of DNA by *Eco*RI could not be resolved. Of particular interest is the identification of those processes which take place after the initial association of enzyme and substrate and before the cleavage of the phosphodiester bond occurs, since these might be correlated with molecular recognition. For this purpose we have started to investigate the kinetics of the interaction of synthetic double-stranded oligonucleotides with *Eco*RI using a fluorescence stopped-flow apparatus. The results of these experiments, together with steady-state cleavage data, demonstrate that (I) *Eco*RI binds to oligodeoxynucleotides containing the recognition site in a nearly diffusion-controlled reaction, (II) recognition and phosphodiester bond cleavage are concerted reactions which cannot be resolved, (III) the intermediate with one phosphodiester bond cleaved can dissociate from the enzyme, and (IV) the rate constants governing the individual reaction steps following complex formation are influenced by the sequence flanking the recognition site.

Experimental Procedures

Materials. The tridekadeoxynucleotides d(TATAGAATTCTAT) and d(TCGCGAATTCGCG) were synthesized on a Biosearch 8600 DNA synthesizer on a 1-μmol scale with β-cyanoethyl phosphoroamidites and tetrazole from Cruachem, acetonitrile (HPLC grade) from Baker, tetrahydrofuran and dichloroethane from Fluka, and all other reagents from Merck. Between 60 and 80 A^{260} units of crude 5′-(dimethoxytrityl)oligodeoxynucleotides was obtained which were purified by reversed-phase high-performance liquid chromatography on a 2.5 × 25 cm LiChrosorb RP-18 column (Merck) with a Bruker LC 21 B liquid chromatograph and a Shimadzu SPD-6A spectrophotometer. Elution was carried out at ambient temperature at a flow rate of 4 mL/min with a linear gradient from 30% to 100% B in 90 min (solvent A: 0.1 M triethylammonium acetate, pH 7.0, 1% acetonitrile; solvent B: 0.1 M triethylammonium acetate, pH 7.0, 50% acetonitrile). The HPLC run was monitored at 290 nm. Oligodexoynucleotides eluting at the end of the gradient producing the dominant UV-absorption peak were collected, taking care to exclude material producing a shoulder ahead

† This work has been supported by grants from the Deutsche Forschungsgemeinschaft (Ma 465/11-5 and Pi 122/2-3) and the Fonds der Chemischen Industrie.
* To whom correspondence should be addressed.

0006-2960/89/0428-7879$01.50/0

and after the major peak. After lyophilization, removal of the dimethoxytrityl group by incubation in 80% acetic acid for 30 min at ambient temperature, extraction with ether, and lyophilization, 6–10 A^{260} units of 95–99% pure tridekadeoxynucleotides was obtained, as determined by analytical reversed-phase HPLC on a 0.46 × 25 cm C4 wide pore column (Baker) with a linear gradient from 10% to 30% B (vide supra) in 20 min at a flow rate of 1 mL/min (Pingoud et al., 1989).

*Eco*RI was isolated from an overproducing strain as described recently (Wolfes et al., 1986) and stored in the presence of 80% (v/v) glycerol in 50 mM Tris-HCl, pH 7.5, 300 mM NaCl, 1 mM EDTA, 0.1 mM 1,4-dithioerythritol, and 0.01% (w/v) Lubrol (Sigma). It was to over 95% pure as determined by polyacrylamide gel electrophoresis in the presence of sodium dodecyl sulfate and equilibrium isoelectric focusing in the presence of 8 M urea. It had a specific activity of 3×10^6 units/mg with bacteriophage λ DNA. *Eco*RI solutions were dialyzed for all experiments against 20 mM Tris-HCl, pH 7.2, 300 mM NaCl, 0.1 mM 1,4-dithioerythritol, and 0.01% (w/v) Lubrol and immediately prior to all experiments diluted to give 20 mM Tris-HCl, pH 7.2, 50 mM NaCl, 10 mM $MgCl_2$ (or 10 mM EDTA), 0.1 mM 1,4-dithioerythritol, and variable amounts of Lubrol.

Steady-State Cleavage Experiments. In order to determine the k_{cat} values for the *Eco*RI-catalyzed cleavage of oligodeoxynucleotides, 0.01–1 μM *Eco*RI and 1–2 μM double-stranded d(TCGCGAATTCGCG) or d(TATAGAATTCTAT), respectively, were incubated in 20 mM Tris-HCl, pH 7.2, 50 mM NaCl, and 10 mM $MgCl_2$ at 25 °C. The reaction was stopped after defined time intervals by addition of excess EDTA. The reaction products were analyzed by reversed-phase high-performance liquid chromatography on a C4 wide pore column (Baker). Separation of substrate and products was achieved with a linear gradient of 5–16% acetonitrile in 0.1 M triethylammonium acetate, pH 7.0, within 22 min at a flow rate of 1 mL/min (Figure 1). High-performance liquid chromatography was carried out on a Merck-Hitachi 655A-12 liquid chromatograph with an L-5000 LC controller, a 655A variable-wavelength UV monitor set at 260 nm, and a D-2000 chromatointegrator.

Fluorescence Stopped-Flow Experiments. Stopped-flow experiments were performed at 25 °C in a modified version of a Durrum-Gibson stopped-flow apparatus. Protein fluorescence was excited at 270 or 280 nm and measured after passage through Schott UG11 and KV320 band-pass filters.

Data were recorded with a personal computer using the Disys PCI analog input cards. Fluorescence amplitudes were measured with the shortest time intervals possible (0.2 ms) and were averaged over continuously increasing time intervals after the experiment. This allows measurement of the pre-steady-state as well as steady-state kinetics in a single experiment. Due to the averaging procedure, the signal to noise ratio of the data increases with increasing time. Figure 4 shows the result of a stopped-flow experiment in four different graphs, making use of the conventional linear time scale. For a complete display of the data that cover the range from 2 ms to 140 s in one graph, it is necessary to use a logarithmic time axis as in Figures 5 and 8 or a variable linear time axis as in Figures 6 and 7. The increase in fluorescence at the end of the recording is due to photo bleaching. Since the fluorescence change was rather small, several experiments were accumulated to reduce noise. Data were transferred to a main-frame computer for further analysis.

The kinetic curves were then evaluated by a nonlinear fitting procedure (Powell, 1965). In this procedure the differential

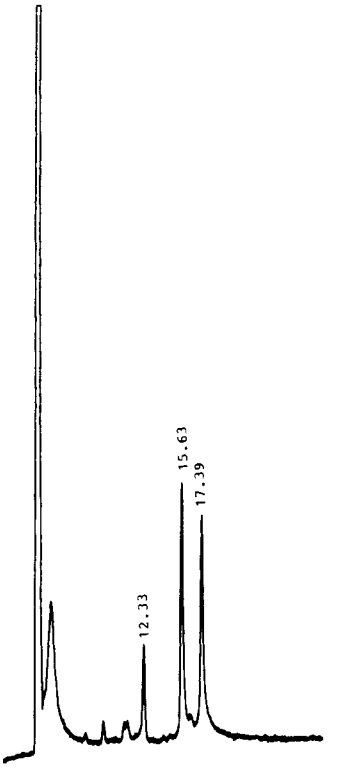

FIGURE 1: HPLC chromatogram of the cleavage of d(TATAGAATTCTAT) by *Eco*RI. 2 μM double-stranded d(TATAGAATTCTAT) was incubated at 25 °C with 0.5 μM *Eco*RI in 20 mM Tris-HCl, pH 7.2, 10 mM $MgCl_2$, and 50 mM NaCl. After 10 s the reaction was stopped by the addition of EDTA and analyzed by reversed-phase HPLC as described under Experimental Procedures. The material eluting after 12.33, 15.63, and 17.39 min represent d(TATAG), d(pAATTCTAT), and d(TATAGAATTCTAT), respectively.

equations describing the change in concentrations of the reactants, intermediates, and products were solved by a multistep predictor corrector method (Gear, 1971). The individual fluxes as defined by the postulated reaction mechanism were calculated by multiplication of the rate constants with the concentrations as shown for Scheme II (the different molecular species are defined under Results). The fluxes are numbered F_1 to F_{13}:

$$F_1 = k_1[E][SS] \quad F_2 = k_{-1}[ESS] \quad F_3 = k_2[ESS]$$
$$F_4 = k_3[ESP] \quad F_5 = k_4[EPP] \quad F_6 = k_5[ESP]$$
$$F_7 = k_{-5}[E][SP] \quad F_8 = k_6[SP] \quad F_9 = k_{-6}[S][P]$$
$$F_{10} = k_8[S][S] \quad F_{11} = k_{-8}[SS] \quad F_{12} = k_7[EP]$$
$$F_{13} = k_{-7}[E][P]$$

The resulting differential equations are the sums of the respective fluxes:

$$d[E]/dt = -F_1 + F_2 + F_5 + F_6 - F_7 + F_{12} - F_{13}$$
$$d[SS]/dt = -F_1 + F_2 + F_{10} - F_{11}$$
$$d[ESS]/dt = +F_1 - F_2 - F_3$$
$$d[ESP]/dt = +F_3 - F_4 - F_6 + F_7$$
$$d[EPP]/dt = +F_4 - F_5$$
$$d[EP]/dt = -F_{12} + F_{13}$$
$$d[SP]/dt = +F_6 - F_7 - F_8 + F_9$$
$$d[S]/dt = +F_8 - F_9 - 2F_{10} + 2F_{11}$$
$$d[P]/dt = +2F_5 + F_8 - F_9 + F_{12} - F_{13}$$

The fluorescence increments for the different species as well as the kinetic constants for the fit with the minimal sum of residual deviations were calculated for the individual experiment. It is also possible to fit a single set of kinetic parameters to several different experiments. The program allows easy incorporation of different mechanisms. The principle of parsimony was used in deciding which mechanism was the best one to describe the stopped-flow data. The reliability of the results of the numerical iteration was checked by carrying out simulations with values for individual rate constants which differ from the values obtained in the best fit and comparing the root mean square deviations of the results of the iteration and the simulation.

Stopped-flow experiments were carried out for the widest range of enzyme concentrations possible, which was determined by the highest concentration at which the *Eco*RI endonuclease does not significantly aggregate under the reaction conditions (i.e., 0.6 μM) and by the lowest concentration at which a fluorescence effect could be reliably detected (i.e., 0.05 μM). The oligonucleotide concentration ranged from equimolar up to an 8-fold excess over enzyme concentration. An excess of enzyme over substrate was avoided in order to prevent a possible self-inhibition of the enzyme (Alves et al., 1982).

Temperature-Jump Experiments. The equilibrium between the single-stranded and double-stranded form of the oligodeoxynucleotides is part of Scheme II. The kinetic constants of such an equilibrium are easily evaluated by relaxation kinetic experiments. Temperature-jump kinetics of oligodeoxynucleotide double-strand formation were measured with a Garching Instruments temperature-jump spectrofluorometer. The relaxation times were determined at different temperatures in the range of double-strand melting. Figure 3 gives the measured relaxation times and amplitudes at different temperatures for d(TATAGAATTCTAT). Assuming a simple bimolecular mechanism

$$2\text{ss-DNA} \underset{k_{-1}}{\overset{k_1}{\rightleftharpoons}} \text{ds-DNA}$$

the relaxation time is given by

$$1/\tau = 2k_1c_{ss} + k_{-1}$$

The free concentrations of single-stranded oligonucleotide were determined for each temperature from the relaxation amplitudes. The kinetic constants gave a linear Arrhenius plot and were extrapolated to the temperature used in the stopped-flow experiments. They were included as independently measured constants in the fitting procedure for Scheme II.

Results

We have selected tridekadeoxynucleotides for our study, since they are sufficiently long to cover the DNA binding site of *Eco*RI (Lu et al., 1981; Frederick et al., 1984) and too short to provide nonspecific binding sites when the specific site is occupied by this enzyme. We have synthesized the palindromic tridekadeoxynucleotides, viz.

d(TATA*GAATTC*TAT)
I

d(TCGC*GAATTC*GCG)
II

which contain the *Eco*RI recognition site but differ in the flanking sequences. Studying the interaction of two oligodeoxynucleotides with *Eco*RI should provide information on whether the effects that we see are modulated by flanking sequences (Alves et al., 1984).

Steady-State Cleavage Experiments. The steady-state as well as the transient kinetics of the *Eco*RI-catalyzed cleavage of high molecular weight DNA, e.g., plasmid DNA, has been studied previously by measuring the disappearance of substrate (supercoiled DNA) and the appearance of product (open circular or linear DNA, respectively) (Langowski et al., 1981; Halford & Johnson, 1983). It is known from these studies that at low enzyme concentrations the association of the enzyme to the specific site is the rate-determining step and that at higher enzyme concentrations, however, the rate of phosphodiester bond cleavage or a rearrangement of the enzyme–substrate complex becomes limiting for the overall reaction.

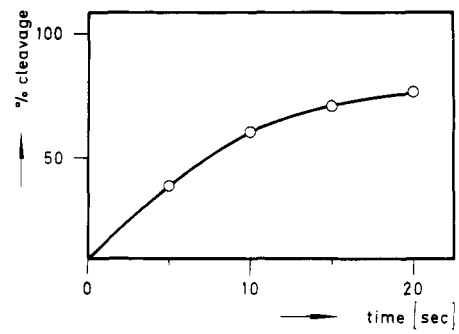

FIGURE 2: Time course of the cleavage of d(TATAGAATTCTAT) by *Eco*RI. 2 μM double-stranded d(TATAGAATTCTAT) was incubated at 25 °C with 0.5 μM *Eco*RI in 20 mM Tris-HCl, pH 7.2, 10 mM $MgCl_2$, and 50 mM NaCl. After 5, 10, 15, and 20 s aliquots were withdrawn. EDTA was added to give a final concentration of 20 mM. The cleavage was analyzed by reversed-phase HPLC (cf. Figure 1). From the slope it is apparent that 0.15 μM double-stranded oligonucleotides are cleaved by 0.5 μM enzyme per second, which corresponds to 0.3 μM double-stranded oligonucleotides (μM enzyme)$^{-1}$ s^{-1} or 0.6 μM phosphodiester bonds (μM enzyme)$^{-1}$ s^{-1}.

In order to correlate effects observed in the fluorescence stopped-flow experiments after mixing of *Eco*RI and oligodeoxynucleotides with steady-state kinetic parameters, we have measured the k_{cat} of the *Eco*RI-catalyzed cleavage of oligodeoxynucleotides by measuring the initial rate at substrate concentrations well above the respective K_M. Figure 2 shows the time course of cleavage of d(TATAGAATTCTAT) with excess substrate. From this and similar experiments the k_{cat} of phosphodiester bond cleavage was determined to be 0.6 s^{-1} for this oligodeoxynucleotide. d(TCGCGAATTCGCG) is cleaved considerably more slowly, k_{cat} being 0.1–0.2 s^{-1}. These results are in agreement with the finding that AT base pairs next to the *Eco*RI recognition site have a favorable effect on the cleavage reaction when compared to GC base pairs (Alves et al., 1984). It should be noted that k_{cat} as determined in these experiments gives only a lower limit for the intrinsic rate of the cleavage of the first phosphodiester bond (k_2 in Figure 9).

Fluorescence Stopped-Flow Experiments. In order to study the time course of the cleavage reaction in more detail and to identify transient intermediates, we have analyzed the processes following rapid mixing of *Eco*RI and various oligodeoxynucleotides using a fluorescence stopped-flow apparatus.

*Eco*RI endonuclease contains 8 tyrosine, 11 phenylalanine, and 2 tryptophan residues (Newman et al., 1981; Greene et al., 1981). Its fluorescence excitation spectrum has a maximum at 280 nm. Excitation at 280 nm, however, gives only very small differences in the fluorescence signal between the free enzyme and the enzyme–oligodeoxynucleotide complex. On the other hand, the fluorescence excited at 270 nm is quenched by 3% upon complex formation. This indicates that the environment of the tyrosine and/or phenylalanine residues is changed with complex formation.

The time course of the fluorescence signal produced after rapid mixing of *Eco*RI and d(TATAGAATTCTAT) in the

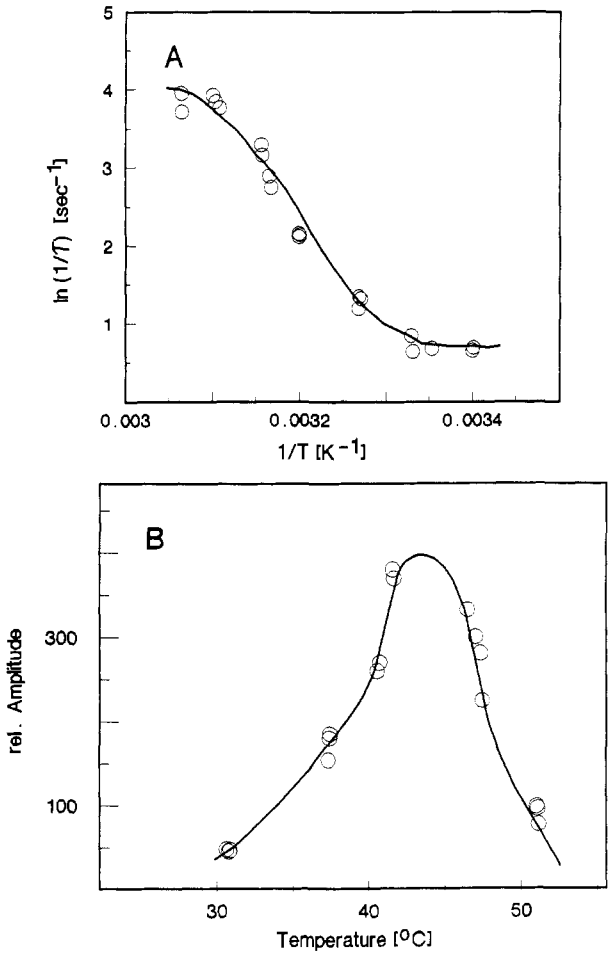

FIGURE 3: Temperature-jump experiments with d(TATAGAATTCTAT). Temperature-jump experiments were carried out with 0.2 μM d(TATAGAATTCTAT) in 20 mM Tris-HCl, pH 7.2, 10 mM $MgCl_2$, and 50 mM NaCl at the temperatures indicated. The temperature dependence of the relaxation times and amplitudes is shown in (A) and (B), respectively. From these data the association and dissociation rate constants for the 2ss ⇌ ds equilibrium can be derived.

presence of Mg^{2+} ions shows several effects (Figures 4 and 5): The reaction is accompanied by a fast decrease in fluorescence in the millisecond time range, followed by a slower and smaller increase in fluorescence within seconds, leading to a plateau which is terminated by an increase in fluorescence. By altering the experimental conditions, it was possible to correlate these different effects to individual processes involved in the enzymatic reaction. The rate of the initial fast decrease in fluorescence is dependent on the concentration of both enzyme and substrate. It represents the bimolecular association of enzyme and substrate. Since the length of the plateau phase depends on the excess of substrate over enzyme (Figure 5D), we assign this phase to the steady state of the reaction. The subsequent increase in fluorescence shows the release of the products from the enzyme and/or a subsequent conformational rearrangement of the enzyme. The slight decrease of the fluorescence (apparently magnified by the logarithmic time scale) superimposed on the overall reaction depends on the intensity of the exciting light and represents a light-induced denaturation of the enzyme. For the evaluation of the stopped-flow experiments, the effects due to light inactivation were subtracted. Figures 6–8 show of stopped-flow experiments in which the fluorescence increase due to photo bleaching had been subtracted. Different from the experiments with equimolar amounts of substrate over enzyme, experiments with a higher excess of substrate give a release phase which is not a single process and, therefore, indicative of a complex reaction mechanism (vide infra).

Fitting of the Stopped-Flow Data. We have analyzed the stopped-flow data in terms of several mechanistic schemes. The most simple kinetic mechanism is shown in Scheme I, where SS represents the double-stranded oligodeoxynucleotide which is cleaved simultaneously in both strands to the product PP (which for the sake of simplicity is indicated as a single species). The dissociation of the product into short single-stranded fragments and binding of the product to the enzyme are not considered. The results of this evaluation are only satisfactory at comparable concentrations of enzyme and substrate. With a high initial excess of substrate over enzyme, the last phase of the reaction could not be fitted (Figure 6), from which we conclude that under these conditions other reactions become significant.

Scheme I

$$E + SS \rightleftharpoons ESS \rightarrow EPP \rightarrow E + PP$$

A realistic alternative to Scheme I is Scheme II, in which both single strands of the double-stranded substrate (SS in Scheme II) are cleaved independently and in which the enzyme can dissociate from the nicked double strand (SP in Scheme II). The nicked double strand when released from the enzyme can dissociate into its fragments (S and P in Scheme II); the uncleaved strand can reassociate with its complementary strand. In this mechanism also binding of the product (P in Scheme II) to the enzyme is considered, which leads to the formation of the complex EP. Product P, therefore, is considered as a weak competitive inhibitor for the cleavage reaction in agreement with previous reports concerning the nonspecific binding of single-stranded oligodeoxynucleotides to *Eco*RI (Goppelt et al., 1980) and their competitive inhibition of the cleavage reaction (Langowski et al., 1980). In experiments where an oligodeoxynucleotide that had been cleaved with *Eco*RI in catalytic amounts was mixed with *Eco*RI in micromolar concentration, there was a very small fluorescence increase of less then 1%, which is taken as direct evidence for the existence of the species EP (data not shown).

Scheme II

$$E + SS \underset{k_{-1}}{\overset{k_1}{\rightleftharpoons}} ESS \xrightarrow{k_2} ESP \xrightarrow{k_3} EPP \xrightarrow{k_4} E + P + P$$

$$ESP \underset{k_{-5}}{\overset{k_5}{\rightleftharpoons}} E + SP$$

$$SP \underset{k_{-6}}{\overset{k_6}{\rightleftharpoons}} S + P$$

$$S + S \underset{k_{-8}}{\overset{k_8}{\rightleftharpoons}} SS$$

$$EP \underset{k_{-7}}{\overset{k_7}{\rightleftharpoons}} E + P$$

The rate constants for formation and dissociation of the double strand, k_8 and k_{-8}, were measured independently in temperature-jump experiments (Figure 3) and were used for the fitting procedure. This mechanism can fit the experimental data obtained with d(TATAGAATTCTAT) over the entire time range and for all oligodeoxynucleotide concentrations. The resulting rate constants are given in Table I. With d(TCGCGAATTCGCG) fewer experiments were carried out than with d(TATAGAATTCTAT); stopped-flow experiments with approximately equimolar concentrations of substrate and enzyme were evaluated, since only in these experiments was the reaction completed within a reasonable time interval. Scheme II can fit also these experimental results, albeit with

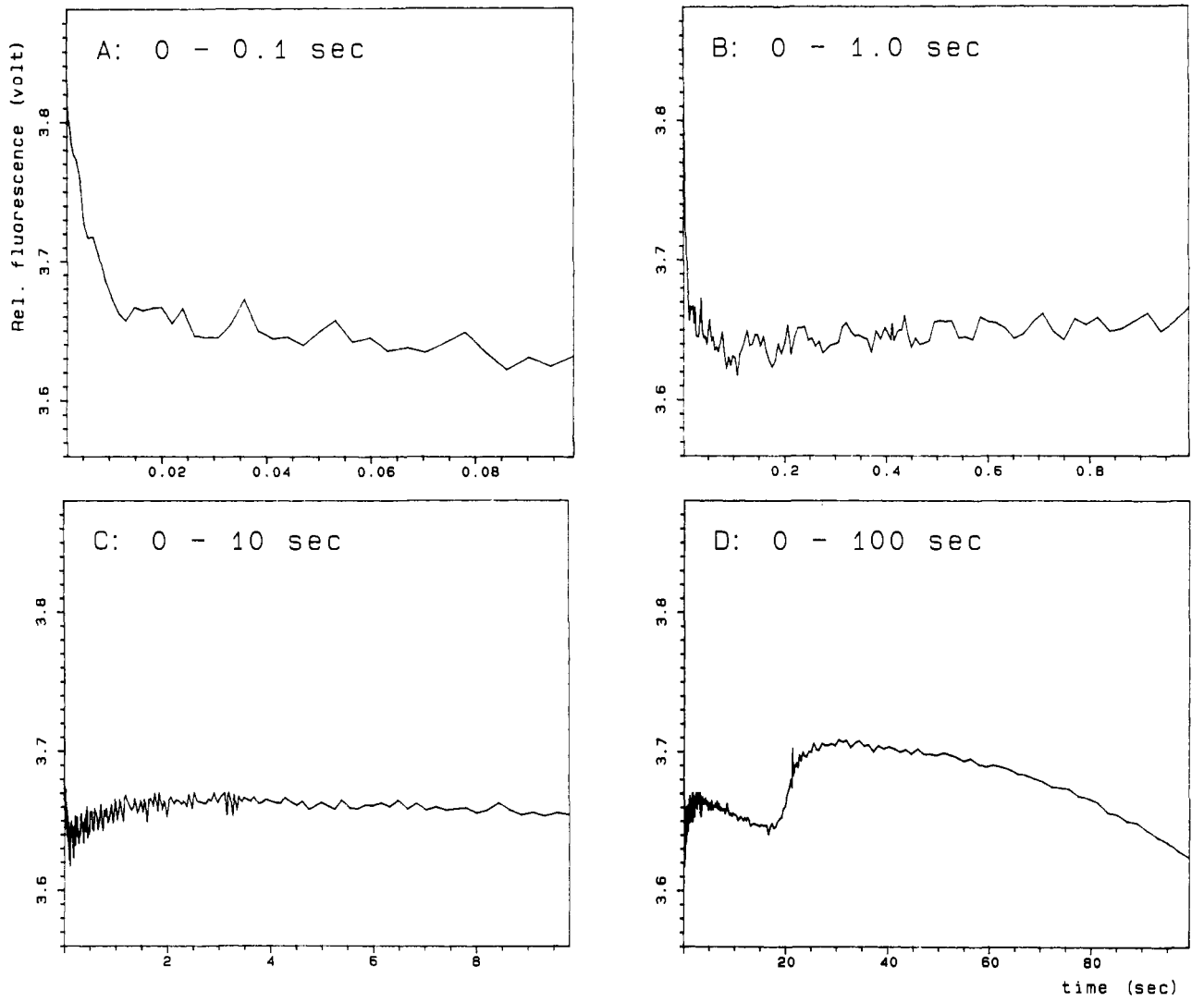

FIGURE 4: Fluorescence stopped-flow kinetics of the cleavage of d(TATAGAATTCTAT) by *Eco*RI. 0.8 μM double-stranded d(TATAGAATTCTAT) was rapidly mixed at 25 °C with 0.2 μM *Eco*RI, both dissolved in 20 mM Tris-HCl, pH 7.2, 10 mM $MgCl_2$, and 50 mM NaCl. The fluorescence of the enzyme was recorded between 2 ms and 140 s after mixing. The time course of the reaction is shown between (A) 0 and 0.1 s, (B) 0 and 1 s, (C) 0 and 10 s, and (D) 0 and 100 s. The information content in these graphs can be conveniently condensed with a variable linear (see Figures 6 and 7) or a logarithmic time scale (see Figures 5 and 8). This data set is one out of 14 which were accumulated and normalized by the number of files incorporated into the composite file which is shown in Figures 5C and 6.

different kinetic constants (Table I).

The comparison of the two sets of rate constants which describe the cleavage of d(TATAGAATTCTAT) and d(TCGCGAATTCGCG) reveals differences which explain why the former oligodeoxynucleotide is processed more quickly by *Eco*RI than the latter one: both oligodeoxynucleotides are bound by the enzyme in the presence of Mg^{2+} ions with high affinity, whose precise magnitude cannot be given, since the stopped-flow experiments could only be carried out at enzyme and substrate concentrations in the micromolar range. The experimental data can be fitted with a binding constant of $\geq 10^8$ M^{-1} for d(TATAGAATTCTAT) and $\geq 3 \times 10^6$ M^{-1} for d(TCGCGAATTCGCG). While for the dissociation rate constant only an upper limit can be given, the association rate constant could be determined accurately: d(TATAGAATTCTAT) is bound in a nearly diffusion-controlled reaction, d(TCGCGAATTCGCG) by about 1 order of magnitude more slowly. This difference is significant and might indicate that d(TCGCGAATTCGCG) cannot adopt as easily as d(TATAGAATTCTAT) the proper conformation to be bound by the enzyme. It could be speculated that this difference reflects the different propensities of the two oligodeoxynucleotides to form the neokinks observed in the cocrystal of *Eco*RI and d(TCGCGAATTCGCG) (Frederick et al., 1984).

The rate of association is not limiting for the cleavage reaction under the concentrations prevailing in the stopped-flow experiments but rather the rate of the catalytic reaction per se as well as the rate of subsequent reactions. d(TATAGAATTCTAT) is cleaved in the first strand by more than a factor of 3 faster than d(TCGCGAATTCGCG). This is in good agreement with the steady-state kinetic data (vide supra). For both oligodeoxynucleotides the dissociation of the nicked intermediate is the preferred reaction over direct conversion to the final product, since dissociation is by a factor of 3 more likely than double-strand cleavage. However, since the nicked double-stranded d(TCGCGAATTCGCG) disproportionates less efficiently than the nicked double-stranded d(TATAGAATTCTAT) to give the original substrate [k_8 being 4×10^4 M^{-1} s^{-1} for d(TCGCGAATTCGCG) and 1×10^7 M^{-1} s^{-1} for d(TATAGAATTCTAT)] and because the rate of reassociation of the intermediate and the enzyme is sufficiently fast [k_{-5} being 6.3×10^6 M^{-1} s^{-1} for d(TCGCGAATTCGCG)], cleavage of d(TATAGAATTCTAT) occurs predominantly via the rearrangement of the intermediate to give a new double-stranded substrate, while

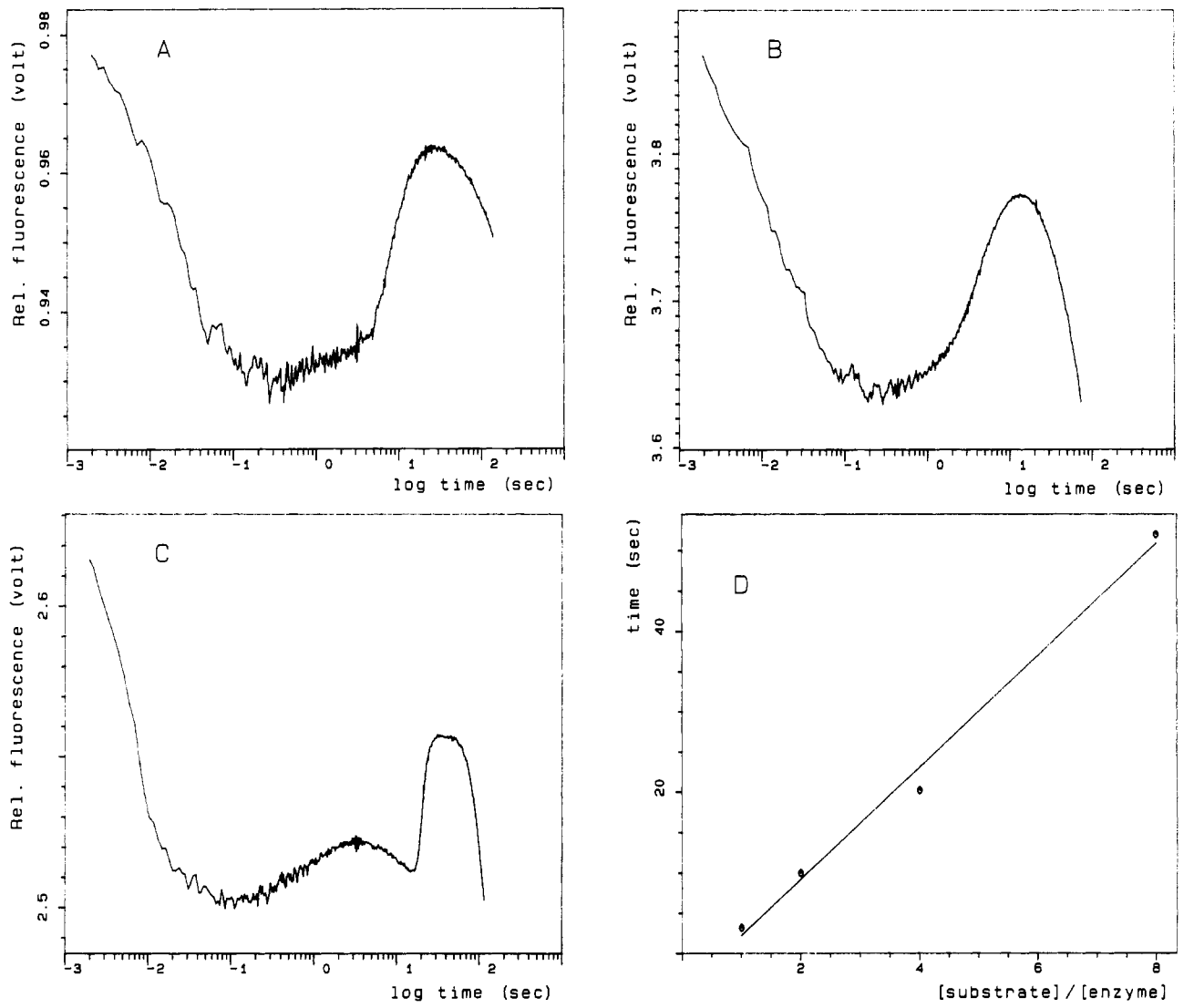

FIGURE 5: Comparison of three different data files recorded for different concentrations of *Eco*RI and d(TATAGAATTCTAT). Double-stranded d(TATAGAATTCTAT) and *Eco*RI, both dissolved in 20 mM Tris-HCl, pH 7.2, 10 mM $MgCl_2$, and 50 mM NaCl, were rapidly mixed in a stopped-flow apparatus at 25 °C. The fluorescence of the enzyme was recorded. These experiments were carried out at different concentrations of enzyme and substrate, respectively. Usually, several experiments were accumulated and normalized to give a composite data file. Concentrations after mixing were (A) 0.05 μM *Eco*RI and 0.1 μM d(TATAGAATTCTAT) (2 experiments), (B) 0.1 μM *Eco*RI and 0.1 μM d(TATAGAATTCTAT) (7 experiments), and (C) 0.1 μM *Eco*RI and 0.4 μM d(TATAGAATTCTAT) (14 experiments). The kinetics are represented with a logarithmic time scale. Differences in the fluorescence are due to different enzyme concentrations and different intensities of the exciting light used in the experiments. (D) The duration of the quasi plateau phase, beginning shortly after mixing of enzyme with substrate and terminated by a sharp rise in fluorescence (time of half maximal amplitude), is plotted versus excess of oligodeoxynucleotide over *Eco*RI. The linear relationship obtained for experiments with the same concentration of enzyme (0.1 μM) and variable amounts of substrate (0.1–0.8 μM) lends credit to our conclusion that the plateau phase represents the quasi steady state of the reaction which begins with the initial complex formation and ends with the consumption of substrate.

cleavage of d(TCGCGAATTCGCG) in both strands occurs to a substantial amount without rearrangement of the nicked double strand. This difference in mechanism is mostly due to the different kinetics with which the nicked double strands rearrange. Limiting for the rearrangement of the GC-rich tridekadeoxynucleotides is the recombination of the uncleaved single strands which has been determined in independent temperature-jump experiments. Since this recombination occurs much more slowly with d(TCGCGAATTCGCG) than with d(TATAGAATCTAT), the former is cleaved in an apparently processive manner, but *not* in a single binding event, while the latter is cleaved distributively. In agreement with this conclusion is our finding that the cleavage of d(TATAGAATTCTAT) by *Eco*RI can be simulated by an obligatory distributive mechanism (k_3 and $k_4 = 0$), while the cleavage of d(TCGCGAATTCGCG) cannot (computer simulations not shown).

Influence of Mg^{2+} Ions on the Mechanism of Oligodeoxynucleotide Cleavage by EcoRI. The experiments described so far were carried out by rapidly mixing solutions of *Eco*RI and the oligodeoxynucleotide in the reaction buffer, viz., 20 mM Tris-HCl, pH 7.2, 50 mM NaCl, and 10 mM $MgCl_2$. Since we also wanted to determine the role of Mg^{2+} in the reaction pathway, we have carried out four types of experiments in which two of the three reaction partners, namely, d(TATAGAATTCTAT), *Eco*RI, and Mg^{2+}, were preincubated in different combinations and then mixed with the third one. The concentrations in the cuvette after rapid mixing were the same in all experiments: 0.2 μM d(TATAGAATTCTAT), 0.1 μM *Eco*RI, and 10 mM Mg^{2+} (Figure 8). Figure 8A shows for reference a set of experiments in which *Eco*RI and d(TATAGAATTCTAT) were mixed with each other in the presence of Mg^{2+}. Mixing an *Eco*RI solution containing Mg^{2+} with a d(TATAGAATTCTAT) solution without Mg^{2+} gave

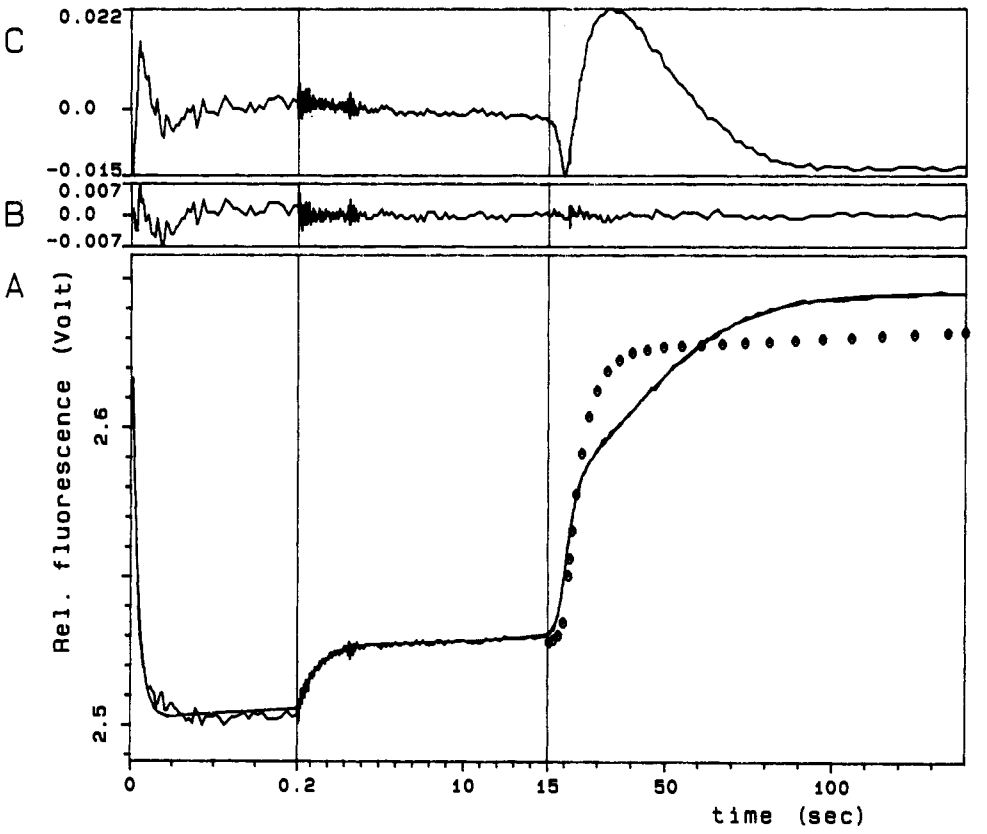

FIGURE 6: Computer fit of the kinetics of cleavage of d(TATAGAATTCTAT) by *Eco*RI. Fourteen individual data files obtained by fluorescence stopped-flow experiments with 0.4 μM (after mixing) double-stranded d(TATAGAATTCTAT) and 0.1 μM (after mixing) *Eco*RI were accumulated and normalized by the number of files. The data are plotted in three time windows with different linear scales. (A) shows the data that are corrected for the amplitude decrease due to bleaching. The continuous line superimposed on the experimental curve represents the fit according to Scheme II. The curve indicated by a discontinuous course of circles (only presented in the third time window) shows the best fit obtained with Scheme I. (B) and (C) are residual plots showing the difference between the experimental time course and the fitted curve for the fit according to Schemes II and I, respectively. The superiority of Scheme II over Scheme I is obvious.

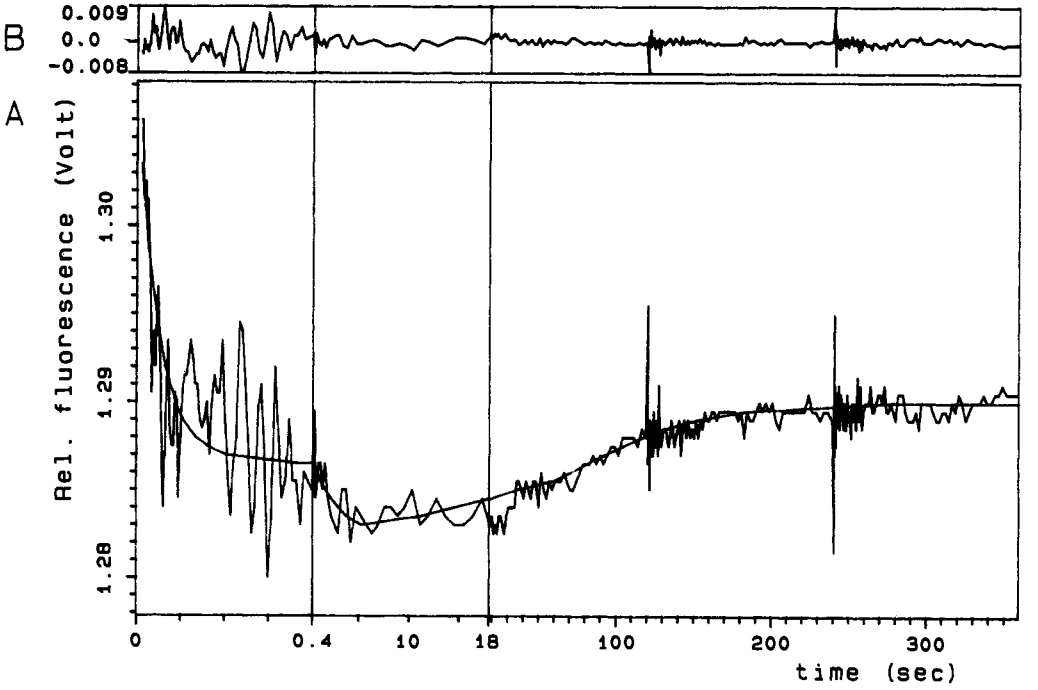

FIGURE 7: Computer fit of the kinetics of cleavage of d(TCGCGAATTCGCG) by EcoRI. Two individual data files obtained by fluorescence stopped-flow experiments with 0.1 μM (after mixing) double-stranded d(TCGCGAATTCGCG) and 0.1 μM (after mixing) *Eco*RI were accumulated and normalized by the number of files. The data are plotted in three time windows with different linear scales. (A) shows the data that are corrected for the amplitude decrease due to bleaching. The continuous line superimposed on the experimental curve represents the fit with Scheme I. (B) is the residual plot showing the difference between the experimental time course and the fitted curve.

a similar result (Figure 8B) as that shown in Figure 8A. Mixing the preformed *Eco*RI/d(TATAGAATTCTAT) complex with Mg^{2+}, however, resulted in an acceleration of the reaction. A fast concentration-dependent fluorescence quench

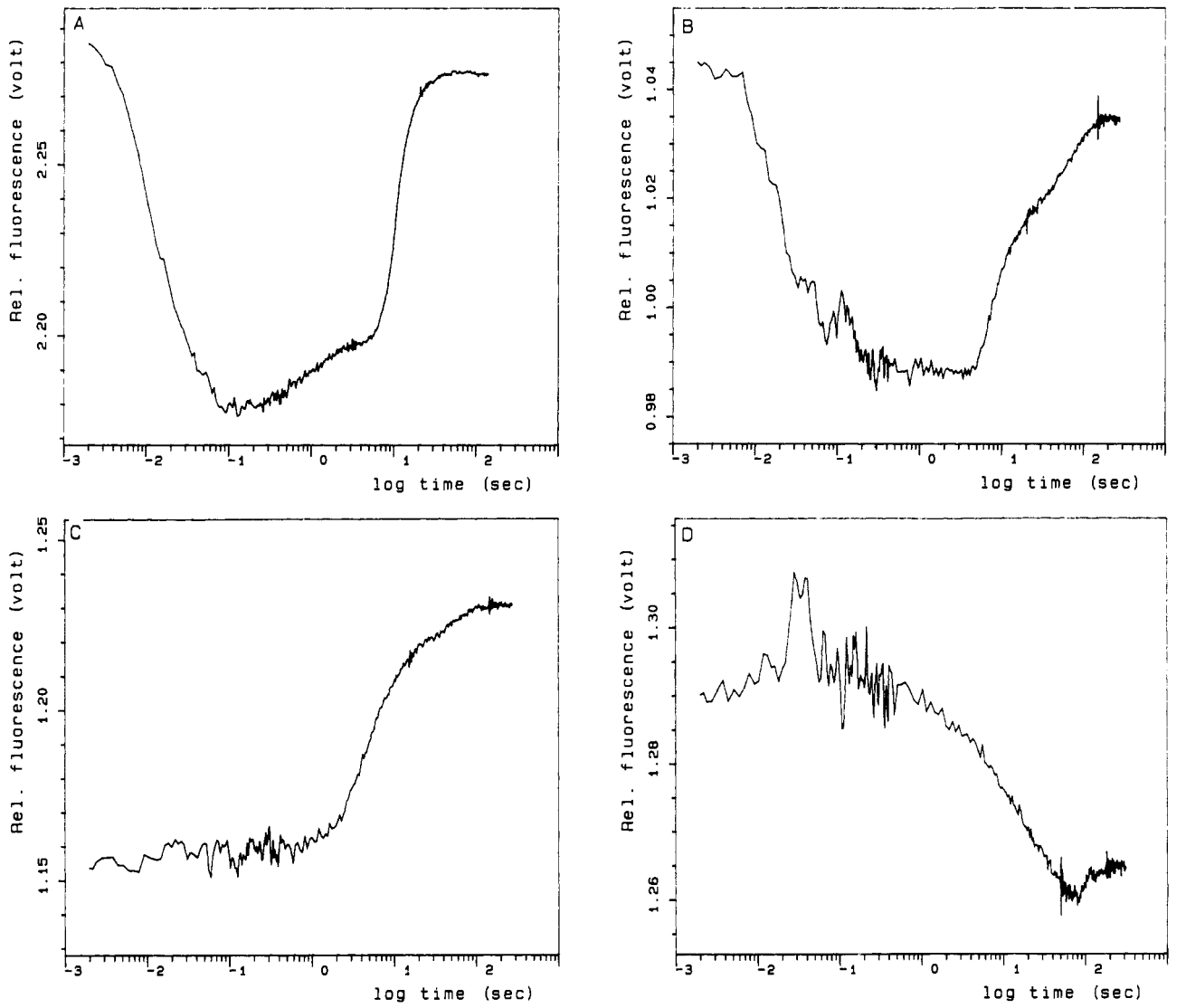

FIGURE 8: Comparison of the fluorescence stopped-flow kinetics of the cleavage of d(TATAGAATTCTAT) by *Eco*RI as measured with different protocols of mixing: (A) *Eco*RI/Mg^{2+} was mixed with d(TATAGAATTCTAT)/Mg^{2+}; (B) *Eco*RI/d(TATAGAATTCTAT) was mixed with Mg^{2+}; (C) *Eco*RI/Mg^{2+} was mixed with d(TATAGAATTCTAT); (D) *Eco*RI was mixed with d(TATAGAATTCTAT)/Mg^{2+}. In all experiments the final concentrations were 0.1 μM *Eco*RI, 0.2 μM d(TATAGAATTCTAT), and 10 mM Mg^{2+} in 20 mM Tris-HCl, pH 7.2, and 50 mM NaCl. The data are corrected for the decrease in amplitude due to bleaching. The signal to noise ratio is quite different in the four sets of experiments, since for (A) 20 individual data files were accumulated while for (B) 3 and for (C) and (D) only 2 stopped-flow experiments were evaluated. Small differences in the fluorescence intensities are due to variations in the excitation light intensity. In all cases the composite data files were normalized by the number of files.

was not observed; the onset of the release phase occurred 3 s earlier (Figure 8C). These results demonstrate that Mg^{2+} associates with the preformed enzyme–substrate complex in a reaction which is too fast to be resolved by our instrument and/or does not change the fluorescence of the enzyme. Mixing d(TATAGAATTCTAT)/Mg^{2+} with *Eco*RI gave a completely different result. There was no fast effect, and the onset of the release phase was shifted to 80 s. This means that the *Eco*RI endonuclease in the absence of the Mg^{2+} and/or DNA adopts an inactive conformation, which is only slowly converted to the catalytically competent state by Mg^{2+} and/or DNA. A similar observation had been made by Halford and Johnson (1983) with single-turnover experiments in which the cleavage of pMB9 DNA by *Eco*RI was monitored with ethidium bromide as a reporter group.

Discussion

We have analyzed by fast kinetic techniques the *Eco*RI-catalyzed cleavage of two synthetic oligodeoxynucleotides carrying the *Eco*RI recognition site but differing in their flanking sequences. Using a novel method of data acquisition over a wide time range, it was possible to record the pre steady state as well as the steady state of the reaction in one experiment. By accumulation of the data of individual experiments carried out at identical conditions, small effects, hitherto not amenable to a reliable measurement, could be assessed. Furthermore, the simultaneous numerical analysis of many experiments carried out with different concentrations of enzyme and substrate under otherwise identical conditions allowed us to formulate a reaction scheme which accurately describes the cleavage of oligodeoxynucleotides by *Eco*RI in terms of reaction rate constants. Figure 9 is a composite albeit minimal diagram of the individual reactions that could be resolved. The salient features of this diagram can be summarized as follows: In the presence of Mg^{2+}, *Eco*RI and tridecadeoxynucleotide substrates associate in a nearly diffusion-controlled reaction. The stability of the resulting complex is high: all reactions could be satisfactorily fitted with K_{assoc} values of 10^6–10^8 M^{-1}, depending on the substrate, but these values constitute lower limits. The 10-fold difference in the

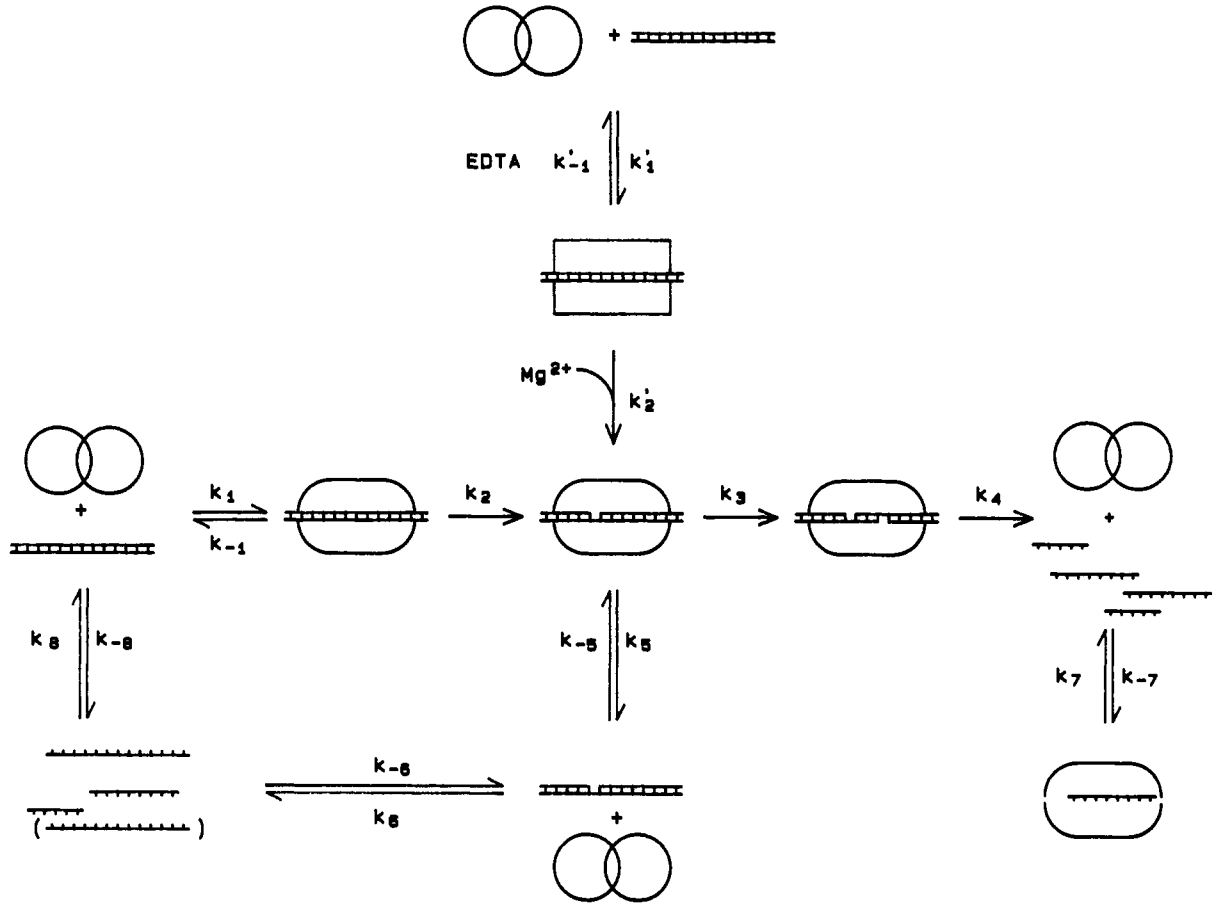

FIGURE 9: Reaction scheme for the cleavage of oligodeoxynucleotides by *Eco*RI. The *Eco*RI dimer in its free state is indicated by two overlapping circles. Upon binding to DNA in the presence of Mg^{2+}, a conformational change of the enzyme occurs; the enzyme is symbolized in the complex by an ellipsoid ring. In the presence of EDTA the binding of DNA does not lead to a catalytically competent complex with DNA; the enzyme in this complex is symbolized by a square. In the presence of Mg^{2+} cleavage of the oligonucleotide occurs, either in both strands in a consecutive reaction or only in one strand. The cleavage reaction is followed by dissociation of the respective products. The nicked double strand when dissociating from the enzyme can rearrange to form a new substrate molecule and reenter into the reaction.

Table I: Results of the Fitting Procedure Using Scheme II[a]

	d(TATAGAATTCTAT)	d(TCGCGAATTCGCG)
k_1 (M^{-1} s^{-1})	3×10^8 ($+2 \times 10^8$, -1×10^8)	4×10^7 ($+0.5 \times 10^7$, -1×10^7)
k_{-1} (s^{-1})[b]	3	14
k_2 (s^{-1})	1.3 (+0.7, −0.3)	0.37 (+0.01, −0.02)
k_3 (s^{-1})	0.057 (+0.003, −0.002)	0.035 (+0.002, −0.005)
k_4 (s^{-1})	0.27 (+0.07, −0.02)	4 (+23, −2)
k_5 (s^{-1})	0.17 (±0.05)	0.139 (+0.001, −0.002)
k_{-5} (M^{-1} s^{-1})	1.2×10^6 ($\pm 0.2 \times 10^6$)	6.3×10^6 ($+0.1 \times 10^6$, -0.7×10^6)
k_6 (s^{-1})	0.0165 (±0.0015)	0.8 (±0.7)
k_{-6} (M^{-1} s^{-1})[b]	1×10^3	4×10^6
k_7 (s^{-1})[b]	0.003	0.16
k_{-7} (M^{-1} s^{-1})[b]	7.10^4	4×10^5
k_8 (M^{-1} s^{-1})[c]	1×10^7	4×10^4
k_{-8} (s^{-1})[c]	0.01	8×10^{-9}

[a] The individual rate constants (cf. Figure 9) were obtained in the best fit of *all* stopped-flow experiments analyzed in a single iteration procedure. Indicated in parentheses is which range will give a ±10% difference of the root mean square deviation, since we estimate that this is the experimental error of the stopped-flow experiments. [b] The absolute values of these rate constants are not critical for the precise fit of the experimental data. The numbers given constitute upper (k_{-1}, k_7) and lower (k_{-6}, k_{-7}) limits, respectively. [c] These constants were determined experimentally in temperature-jump experiments.

association rate constants of the two different oligodeoxynucleotides suggests that the association reaction might involve an adaptation of the substrate to the surface of the enzyme, possibly a kinking of the phosphodiester backbone, whose rate depends on the nucleotide sequence adjacent to the recognition site. There is no spectroscopic evidence for a conformational change of enzyme or substrate prior to the cleavage of the first phosphodiester bond. This result leads to the conclusion that in the presence of Mg^{2+} the recognition process is intimately involved with the catalytic reaction. Such a concerted mechanism precludes the kinetic resolution of individual conformational transitions for which evidence exists from structural studies both in the crystal (Frederick et al., 1984) and in solution (Kim et al., 1984) which were carried out, however, under conditions where cleavage does not occur. The concerted transition from binding to catalysis which occurs in the presence of Mg^{2+} might indicate that the distinction between catalytic groups and binding groups is to some degree arbitrary [cf. Kraut (1988) and Carter and Wells (1988)].

Since an enzyme–substrate complex formed in the absence

of the essential cofactor Mg^{2+} leads to a faster cleavage reaction upon addition of Mg^{2+} than observed upon mixing enzyme and substrate in the presence of Mg^{2+}, we conclude that this preformed complex has already undergone some of the conformational transitions needed for catalysis to take place. Halford and Johnson (1983) arrived at a similar conclusion on the basis of the results of single-turnover experiments with *Eco*RI and plasmid DNA.

*Eco*RI cleaves substrates with different sequences flanking the recognition site with different k_{cat} (Alves et al., 1984; this work). This can now be explained in terms of differences in the individual rate constants governing the partial reactions of the cleavage process. Under conditions where association of enzyme and substrate is not limiting, the reaction which seems to be most sensitive to differences in sequence is the cleavage of the first phosphodiester bond. After the cleavage of the first phosphodiester bond (cleavage in one strand), the nicked double strand can dissociate from the enzyme or can be further processed by the enzyme to give the final product (cleavage in both strands). The rate constants of these two alternative reactions are slightly different for different substrates. This is in agreement with previously published results obtained with plasmid DNAs which showed that depending on the substrate and the reaction conditions a nicked intermediate, i.e., open circular DNA, may accumulate. If dissociation of the intermediate occurs (Ruben et al., 1977; Rubin & Modrich, 1978; Halford et al., 1979), it can reassociate with the enzyme, which is the likely event for a macromolecular substrate, or alternatively, as is the case for palindromic oligodeoxynucleotides, it can rearrange to reproduce a double-stranded substrate.

In conclusion, we have established a minimal mechanism that describes the individual reactions which play a role in the cleavage of oligodeoxynucleotide substrates by *Eco*RI. This scheme, provided it is extended to account for linear diffusion of the enzyme along the DNA, is sufficiently general to describe also the cleavage of macromolecular DNA by this enzyme.

Acknowledgments

We are indebted to Dr. F. Peters and K. Stieglitz for their assistance in the numerical analysis. The expert technical assistance of K. Zander and R. Mull-Grotefend is gratefully acknowledged. We thank E. Schuchardt and A. Meyer for typing the manuscript.

References

Alves, J., Pingoud, A., Langowski, J., Urbanke, C., & Maass, G. (1982) *Eur. J. Biochem. 124*, 139–142.

Alves, J., Pingoud, A., Haupt, W., Langowski, J., Peters, F., Maass, G., & Wolff, C. (1984) *Eur. J. Biochem. 140*, 83–92.

Berkner, K. L., & Folk, W. R. (1983) *Anal. Biochem. 129*, 446–456.

Brennan, C. A., van Cleve, M. D., & Gumport, R. I. (1986) *J. Biol. Chem. 261*, 7270–7278.

Carter, P., & Wells, J. A. (1988) *Nature 332*, 564–568.

Ehbrecht, H.-J., Pingoud, A., Urbanke, C., Maass, G., & Gualerzi, C. (1985) *J. Biol. Chem. 260*, 6160–6166.

Fliess, A., Wolfes, H., Rosenthal, A., Schwellnus, K., Blöcker, H., Frank, R., & Pingoud, A. (1986) *Nucleic Acids Res. 14*, 4363–3474.

Forsblom, S., Rigler, R., Ehrenberg, M., Petterson, U., & Philipson, L. (1976) *Nucleic Acids Res. 3*, 3255–3269.

Frederick, C. A., Grable, J., Melia, M., Samudzi, C., Jen-Jacobsen, L., Wang, B.-C., Greene, P. J., Boyer, H. W., & Rosenberg, J. M. (1984) *Nature 309*, 327–331.

Gear, C. W. (1971) *Comm. ACM 14*, 185–189.

Goldstein, K., Thomas, M., & Davis, R. W. (1975) *Virology 66*, 420–427.

Goppelt, M., Pingoud, A., Maass, G., Mayer, H., Köster, H., & Frank, R. (1980) *Eur. J. Biochem. 104*, 101–107.

Greene, P. J., Gupta, M., & Boyer, H. W. (1981) *J. Biol. Chem. 256*, 2143–2151.

Halford, S. E., & Johnson, N. P. (1983) *Biochem. J. 211*, 405–415.

Halford, S. E., Johnson, N. P., & Grinsted, J. (1979) *Biochem. J. 179*, 353–365.

Halford, S. E., Johnson, N. P., & Grinsted, J. (1980) *Biochem. J. 191*, 581–592.

Hedgepeth, J., Goodman, H. M., & Boyer, H. W. (1972) *Proc. Natl. Acad. Sci. U.S.A. 69*, 3448–3452.

Jack, W. E., Terry, B. J., & Modrich, P. (1982) *Proc. Natl. Acad. Sci. U.S.A. 79*, 4010–4014.

Kim, R., Modrich, P., & Kim, S.-H. (1984) *Nucleic Acids Res. 12*, 7285–7292.

Kraut, J. (1988) *Science 242*, 533–540.

Langowski, J., Pingoud, A., Goppelt, M., & Maass, G. (1980) *Nucleic Acids Res. 8*, 4727–4736.

Langowski, J., Urbanke, C., Pingoud, A., & Maass, G. (1981) *Nucleic Acids Res. 9*, 3483–3490.

Lu, A.-L., Jack, W. E., & Modrich, P. (1981) *J. Biol. Chem. 256*, 13200–13206.

McClarin, J. A., Frederick, C. A., Wang, B.-C., Greene, P., Boyer, H. W., Grable, J., & Rosenberg, J. M. (1986) *Science 234*, 1526–1541.

McLaughlin, L. W., Benseler, F., Graeser, E., Piel, N., & Scholtissek, S. (1987) *Biochemistry 26*, 7238–7245.

Modrich, P., & Zabel, D. (1976) *J. Biol. Chem. 251*, 5866–5876.

Modrich, P., & Roberts, R. J. (1982) in *Nucleases* (Linn, S. M., & Roberts, R. J., Eds.) pp 109–154, Cold Spring Harbor Laboratory, Cold Spring Harbor, NY.

Newman, A. K., Rubin, A., Kim, S. H., & Modrich, P. (1981) *J. Biol. Chem. 256*, 2131–2139.

Pingoud, A., Fliess, A., & Pingoud, V. (1989) in *HPLC of Macromolecules—A Practical Approach* (Oliver, R. W. A., Ed.) pp 183–208, IRL Press, Oxford.

Powell, M. J. D. (1965) *Comp. J. 7*, 303–307.

Rubin, R. A., & Modrich, P. (1978) *Nucleic Acids Res. 5*, 2991–2997.

Ruben, G., Spielman, P., Tu, C. D., Jay, E., Siegel, B., & Wu, R. (1977) *Nucleic Acids Res. 4*, 1803–1813.

Seela, F., & Kehne, A. (1987) *Biochemistry 26*, 2232–2238.

Terry, B. J., Jack, W. E., Rubin, R. A., & Modrich, P. (1983) *J. Biol. Chem. 258*, 9820–9825.

Terry, B. J., Jack, W. E., & Modrich, P. (1985) *J. Biol. Chem. 260*, 13130–13137.

Thomas, M., & Davis, R. W. (1975) *J. Mol. Biol. 91*, 315–328.

Wolfes, H., Alves, J., Fliess, A., Geiger, R., & Pingoud, A. (1986) *Nucleic Acids Res. 14*, 9063–9080.

Woodhead, J. L., & Malcolm, A. D. B. (1980) *Nucleic Acids Res. 8*, 389–395.